BIOCHEMISTRY
including biophysical chemistry & molecular biology

Article

pubs.acs.org/biochemistry

# Molecular Determinants of Polyubiquitin Recognition by Continuous Ubiquitin-Binding Domains of Rad18

Trung Thanh Thach, Namsoo Lee, Donghyuk Shin, Seungsu Han, Gyuhee Kim, Hongtae Kim, and Sangho Lee*

Department of Biological Sciences, Sungkyunkwan University, Suwon 440-746, Korea

Supporting Information

**ABSTRACT:** Rad18 is a key factor in double-strand break DNA damage response (DDR) pathways via its association with K63-linked polyubiquitylated chromatin proteins through its bipartite ubiquitin-binding domains UBZ and LRM with extra residues between them. Rad18 binds K63-linked polyubiquitin chains as well as K48-linked ones and monoubiquitin. However, the detailed molecular basis of polyubiquitin recognition by UBZ and LRM remains unclear. Here, we examined the interaction of Rad18(201−240), including UBZ and LRM, with linear polyubiquitin chains that are structurally similar to the K63-linked ones. Rad18(201−240) binds linear polyubiquitin chains ($Ub_2$−$Ub_4$) with affinity similar to that of a K63-linked one for diubiquitin. *Ab initio* modeling suggests that LRM and the extra residues at the C-terminus of UBZ (residues 227−237) likely form a continuous helix, termed the "extended LR motif" (ELRM). We obtained a molecular envelope for Rad18 UBZ-ELRM:linear $Ub_2$ by small-angle X-ray scattering and derived a structural model for the complex. The Rad18:linear $Ub_2$ model indicates that ELRM enhances the binding of Rad18 with linear polyubiquitin by contacting the proximal ubiquitin moiety. Consistent with the structural analysis, mutational studies showed that residues in ELRM affect binding with linear $Ub_2$, not monoubiquitin. *In cell* data support the idea that ELRM is crucial in the localization of Rad18 to DNA damage sites. Specifically, E227 seems to be the most critical in polyubiquitin binding and localization to nuclear foci. Finally, we reveal that the ubiquitin-binding domains of Rad18 bind linear $Ub_2$ more tightly than those of RAP80, providing a quantitative basis for blockage of RAP80 at DSB sites. Taken together, our data demonstrate that Rad18(201−240) forms continuous ubiquitin-binding domains, comprising UBZ and ELRM, and provides a structural framework for polyubiquitin recognition by Rad18 in the DDR pathway at a molecular level.

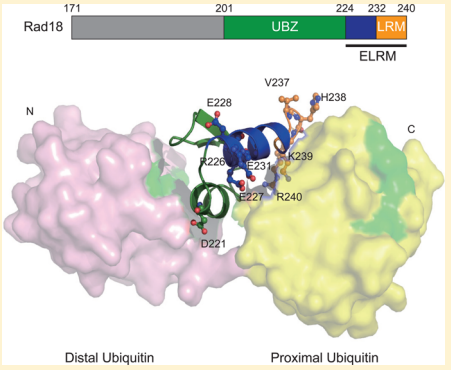


Protein ubiquitylation is an emerging post-translational modification regulating a range of intracellular processes beyond the canonical function of proteasomal protein degradation.[1−4] Ubiquitylation involves covalent attachment of one or more 76-residue ubiquitin moieties to Lys residues of the target protein by a series of enzymes termed E1 ubiquitin-activating enzymes, E2 ubiquitin-conjugating enzymes, and E3 ubiquitin ligases. In the case of polyubiquitylation, multiple ubiquitin moieties form a chain, linked by a specific Lys residue among seven such residues on ubiquitin. Linkage-specific polyubiquitin chains are known to be involved in different biological processes. For example, K63-linked polyubiquitins are associated with DNA damage repair and other signaling processes, while K48-linked ones are associated with canonical cytoplasmic protein degradation.[5] Linear or M1-linked ones have been reported to function in a fashion similar to that of K63-linked ones. Such covalently attached ubiquitin chains are recognized noncovalently by a variety of proteins harboring ubiquitin-binding domains.[5−7]

The DNA damage response (DDR) pathway at double-strand break (DSB) sites is one of the intracellular processes regulated by ubiquitylation.[2] DNA damage can lead to mutations and genomic instability, resulting to tumorigenesis and cell death. Rad18, an E3 ubiquitin ligase and a ubiquitin-binding protein, functions in DNA damage bypass and postreplication in yeast and vertebrates. As an E3 ubiquitin ligase, Rad18 promotes monoubiquitylation of proliferating cell nuclear antigen at stalled replication forks.[8−10] Mouse and chicken cells lacking Rad18 show sensitivity to various DNA-damaging agents and enhanced genomic instability.[11,12] As a ubiquitin-binding protein, Rad18 binds directly to K63-linked polyubiquitin chains and recruits Rad51C to DNA damage sites, facilitating homologous recombination repair.[13] A ubiquitin-binding domain of Rad18 prevents the recruitment of other DDR mediators such as 53BP1, RAP80, and BRCA1 to DSB sites by blocking access of these proteins to ubiquitylated chromatin.[14]

Rad18 harbors multiple domains. At the N-terminus, there is a RING domain (residues 25−64; human numbering) typical of E3 ubiquitin ligases. The C-terminal region contains two domains responsible for binding Rad6 (residues 340−395) and

**Received:** October 4, 2014
**Revised:** February 10, 2015
**Published:** March 10, 2015





DOI: 10.1021/bi5012546
*Biochemistry* 2015, 54, 2136−2148

polymerase $\eta$ (residues 401−445).[15] The UBZ domain (ubiquitin-binding zinc finger; residues 201−224) and SAP domain (SAF-A/B, Acinus, and Pias; residues 243−282) are located in the middle. The SAP domain serves as a DNA-binding domain.[15]

The region including the UBZ domain (residues 186−240) is responsible for ubiquitin recognition in both intra- and intermolecular interactions.[13] Rad18 undergoes monoubiquitylation, and the monoubiquitylated Rad18 is the major form in the cytoplasm.[16] Intramolecular interaction between the monoubiquitin moiety of Rad18 and the UBZ domain is required for Rad18 automonoubiquitylation.[16] The UBZ domain is also involved in targeting Rad18 to DSB sites via a direct interaction with polyubiquitin[13] and localizing Rad18 in nuclei by recognizing ubiquitylated chromatin proteins,[13,17] such as H2A/X.[18,19]

Biochemical and structural characterizations of Rad18 UBZ have advanced recently. The UBZ domain of Rad18 is a type 4 C2HC zinc finger. A recent NMR structure of the Rad18 UBZ domain (residues 198−227) revealed a $\beta1-\beta2-\alpha$ fold.[20] Binding of Rad18 UBZ to monoubiquitin is mediated by hydrophobic interactions of residues in strand $\beta1$ and the $\alpha$-helix as well as electrostatic ones, including D221 of Rad18, a conserved residue among type 3 and 4 UBZ domains (UBZ3 and UBZ4, respectively). UBZ4 from Rad18 binds monoubiquitin with an apparently moderate affinity ($K_d$) of 42 $\mu$M *in vitro*, while $K_d$ values of UBZ4 from Wrnip1 and UBZ3 from polymerase $\eta$ are 37 and 81 $\mu$M, respectively.[15,17,21] Rad18 UBZ binds linkage-specific polyubiquitin chains, K63-linked and K48-linked ones, with different affinities: $K_d$ values of 30 $\mu$M for K63-$Ub_2$ and 106 $\mu$M for K48-$Ub_2$.[17] Binding affinities of Rad18 UBZ with longer polyubiquitin chains increase regardless of linkage specificity: 17 nM for K63-$Ub_5$ and 36 nM for K48-$Ub_5$.[13] However, no information about the binding of Rad18 with other linkage-specific polyubiquitin chains has been reported.

A recent study reveals that the minimal ubiquitin-binding region consists of residues 201−232, a few extra residues beyond the C-terminus of the UBZ domain (residues 201−224).[22] A sequence motif adjacent to the C-terminus of UBZ domain, called the LR motif (LRM; residues 232−240), enhances ubiquitin recognition and provides specificity among other ubiquitin-binding proteins involved in the DSB response.[22] LRM is required for the recruitment of Rad18 to nuclear foci, presumably by participating in recognizing polyubiquitylated proteins localized in the nuclear foci. These reports suggest that the two ubiquitin-binding domains of Rad18, UBZ and LRM, mediate ubiquitin recognition together. Overexpression of UBZ-LRM reportedly suppresses the association of 53BP1, RAP80, and BRCA1 with DSB sites via blockage of K63-linked polyubiquitin moieties of chromatin proteins.[14] This suggests that there may be competition in binding polyubiquitin moieties of the chromatin proteins among proteins involved in the DSB pathway. However, molecular details of the interaction of UBZ-LRM with ubiquitin and blockage of other ubiquitin-binding proteins at DSB sites by UBZ-LRM remain poorly understood.

To obtain mechanistic insights into and functions of ubiquitin recognition by the UBZ-LRM of Rad18 at the molecular level, we investigated which residue(s) contributed to binding ubiquitin quantitatively. Furthermore, we derived a molecular model for Rad18:linear $Ub_2$ in solution by small-angle X-ray scattering combined with molecular modeling. The recruitment of Rad18 to DNA damage sites through polyubiquitin recognition by a new region, termed ELRM, was also examined. Finally, the competitive binding to linear polyubiquitin between Rad18 and RAP80 was monitored quantitatively. Collectively, our results provide insight into how Rad18 recognizes polyubiquitin and functions in the DDR pathway at a molecular level.

## MATERIALS AND METHODS

**Plasmids, Cloning, and Mutagenesis.** Genes encoding various regions of Rad18 were amplified by polymerase chain reaction from full-length human Rad18 cDNA (accession number NM_020165.3) and then inserted between *Bam*HI and *Eco*RI restriction enzyme sites in a parallel GST2 vector.[23] Genes encoding hexahistidine-tagged monoubiquitin (Ub) or linear $Ub_2$, $Ub_3$, or $Ub_4$ were inserted between the *Bam*HI and *Eco*RI sites in a parallel His2 vector. To prepare plasmids encoding monoubiquitin mutants for linkage-specific polyubiquitin synthesis (77D, K63C, and K48C), the gene encoding monoubiquitin was cloned into pET-3a (Novagen) using restriction enzymes *Nde*I and *Eco*RI, and the resulting plasmid was then subjected to site-directed mutagenesis. To express Rad18 UBZ-ELRM constructs in mammalian cells, Rad18(171−240) fused with SV40 nuclear localization signal was cloned into the pEGFP-C2 vector (Clonetech) between *Eco*RI and *Bam*HI restriction enzyme sites. The resulting plasmid, pEGFP-Rad18(171−240)-SV40NLS, encodes EGFP-Rad18(171−240)-linker (GG)-SV40NLS (PKKKRKV) fusion protein. Site-directed mutagenesis was performed with the QuikChange kit (Stratagene) based on the protocol supplied. The identities of all constructs were confirmed by DNA sequencing.

**Protein Expression and Purification.** Linear polyubiquitin chains in which the C-terminal G76 of the preceding ubiquitin moiety is directly linked to the N-terminal M1 of the next ubiquitin moiety were expressed as hexahistidine-tagged proteins: His-$Ub_2$, His-$Ub_3$, and His-$Ub_4$. Rad18 was expressed as a GST fusion protein. All proteins, including Rad18 mutants, were overexpressed in *Escherichia coli* strain BL21(DE3). Cells were inoculated in LB medium, incubated with gentle shaking at 37 °C up to an $OD_{600}$ of 0.8−1.0, induced with 500 $\mu$M isopropyl D-thiogalactoside, and grown further, overnight at 20 °C. The cells were harvested by centrifugation (13000 rpm for 1 h), resuspended in buffer A [50 mM Tris-HCl (pH 7.5) and 150 mM NaCl], and lysed by sonication. The supernatant fraction was applied to glutathione-agarose resin (GE Healthcare) for GST fusion proteins and Ni-NTA-agarose resin (Qiagen) for His-tagged proteins and then eluted in buffer B [50 mM Tris-HCl (pH 8.0) and 10 mM reduced glutathione] or buffer C [50 mM Tris-HCl (pH 7.5), 20 mM imidazole, and 500 mM NaCl]. GST and the His tag were cleaved from the fusion proteins by using tobacco etch virus protease[24] and dialyzing the solution containing the fusion proteins against buffer D [50 mM Tris-HCl (pH 7.5), 150 mM NaCl, and 0.5 mM EDTA]. The released GST or His tag was cleared using glutathione-agarose or Ni-NTA-agarose resin again. Proteins were further purified on a Superdex-75 size exclusion column (GE HealthCare) pre-equilibrated with buffer A. Fractions containing pure proteins, judged by sodium dodecyl sulfate−polyacrylamide gel electrophoresis (SDS−PAGE), were pooled and concentrated by centrifugation through 10 kDa centrifugal filters (Ambicom Ultra). The protein concentration was determined by measuring the absorbance at 280 nm and the Bradford assay.[25]

Proteins required for synthesizing K63- and K48-linked diubiquitin chains were prepared as follows. GST-HIP2 and the


DOI: 10.1021/bi5012546
*Biochemistry* 2015, 54, 2136−2148

GST-Mms2/His-Ubc13 complex were overexpressed in *E. coli* BL21(DE3) cells and purified as described above. The ubiquitin mutants (77D, K63C, and K48C) were overexpressed in *E. coli* BL21(DE3) cells. After lysis, the supernatant was heated at 70 °C for 10 min and then further purified on a Superdex-75 size exclusion column pre-equilibrated with buffer A, supplemented with 1 mM DTT. His-Uba1 was overexpressed in a baculovirus-infected Sf9 insect cell system (Invitrogen). Cells were harvested by centrifugation, resuspended in buffer E [50 mM Tris-HCl (pH 8.0), 200 mM NaCl, 5 mM $\beta$-mercaptoethanol, 5% (v/v) glycerol, and 1× protease inhibitor cocktail (Roche)], and lysed by sonication. His-Uba1 was eluted from the Ni-NTA resin in buffer E containing 40 mM imidazole. Further purification was conducted on a Mono Q anion exchange column (GE Healthcare) equilibrated with buffer F [50 mM Tris-HCl (pH 8.0), 1 mM DTT, and 5% glycerol]. Fractions containing pure His-Uba1 were pooled, concentrated, and stored at −80 °C until they were used.

**K63- and K48-Linked Diubiquitin Synthesis and Purification.** K63- and K48-linked diubiquitin chains were synthesized as reported previously.[26,27] K63-$Ub_2$ was synthesized using the GST-Mms2/His-Ubc13 complex, while GST-HIP2 was used as E2 for K48-$Ub_2$ synthesis. Mammalian E1, His-Uba1, was used in both cases. To synthesize K63-$Ub_2$, 5× reaction buffer was prepared [250 mM Tris-HCl (pH 7.5), 50 mM creatine phosphate, 125 mM $MgCl_2$, 15 IU/mL creatine phosphokinase, 15 IU/mL inorganic pyrophosphate, 300 mM ATP, and 2.5 mM DTT]. A reaction mixture containing 20 mg/mL Ub-77D and 50 mg/mL Ub-K63C with 1× reaction buffer was supplemented with 8 mM GST-Mms2/His-Ubc13 complex and 100 $\mu$M His-Uba1. The solution was incubated at 37 °C for 5 h while being gently shaken. K48-$Ub_2$ was generated similarly. The reaction mixture contained 20 mg/mL Ub-77D, 50 mg/mL Ub-K48C, 50 $\mu$M GST-HIP2, and 100 $\mu$M His-Uba1 in 1× reaction buffer.

Diubiquitin chains were purified by 10-fold dilution of reaction mixtures in 0.5 M ammonium acetate (pH 4.5). Then, the acidified solutions were applied to a cation exchange Hitrap SH column (GE Healthcare) pre-equilibrated with buffer G. Bound proteins were eluted with a linear gradient of buffers G [50 mM ammonium acetate (pH 4.5)] and H [50 mM ammonium acetate (pH 4.5) and 1 M NaCl]. Fractions containing linkage-specific diubiquitin chains were pooled, concentrated, and applied to a Superdex-75 size exclusion column (GE Healthcare) pre-equilibrated with buffer A.

**GST Pull-Down.** Next, 2 $\mu$g of each GST-Rad18 protein was incubated with 40 $\mu$L of glutathione-agarose resin for 30 min at ambient temperature in buffer A and washed three times with the same buffer to remove unbound proteins. Subsequently, 500 ng of polyubiquitin chains was added to the resin bound with GST-Rad18 protein. The mixture was then incubated for 2 h at 4 °C while being gently shaken and washed with buffer I [50 mM Tris-HCl (pH 7.5), 300 mM NaCl, and 0.5% NP-40]. Bound polyubiquitin chains were analyzed by SDS−PAGE and immunoblotting using mouse monoclonal anti-ubiquitin combined with IgG-HRP antibodies or GST-HRP antibodies (Santa Cruz Biotechnology). Protein bands were visualized with an ImageQuant LAS 40 digital system (GE Healthcare).

**Biolayer Interferometry.** Biolayer interferometry (BLI) experiments were performed on a Blitz system (ForteBio). For linkage-specific diubiquitin binding to Rad18, either 1 $\mu$M linear, K48-linked, or K63-linked $Ub_2$ was immobilized on amine reactive sensors (ForteBio). Binding was monitored by adding varying concentrations of GST-Rad18 proteins (0.263−21 $\mu$M) in MES (pH 6.0). To study length-dependent binding of linear polyubiquitin chains to Rad18, His-Ub, His-$Ub_2$, His-$Ub_3$, and His-$Ub_4$ (1 $\mu$M each) were immobilized on Ni-NTA biosensors (ForteBio). Binding of GST-Rad18 proteins (0.263−105 $\mu$M) to the immobilized linear polyubiquitin chains was then monitored. GST was used as a negative control. Experiments were repeated at least twice. The $K_d$ was determined on the basis of steady-state analysis using *PRISM* (GraphPad Software).

***Ab Initio* Modeling of Rad18(201−240).** *Ab initio* models for Rad18(201−240) were derived using *GalaxyTBM*[28] and *Rosetta*.[29] For modeling with *GalaxyTBM*, 100 models that maximally satisfied the restraints were generated within a root-mean-square deviation (rmsd) of 1 Å. A representative structure is the nearest model to the largest cluster center. For *Rosetta* modeling, initially, 20000 models were generated. Then, 1044 structural models within a rmsd of 1 Å were clustered, and the top model from the cluster was selected for further structural analysis. Calculations were performed at the Cassini cluster system at the UCLA-DOE Computer Core facility.

**Small-Angle X-ray Scattering.** Small-angle X-ray scattering (SAXS) experiments were conducted at beamline 4C in the Pohang Accelerator Laboratory (Pohang, South Korea). Data were collected at sample concentrations of 3.91, 1.95, and 0.98 mg/mL in buffer containing 50 mM Tris-HCl (pH 7.5), 150 mM NaCl, and 0.5 mM ethylenediaminetetraacetic acid (EDTA). Final scattering data were generated by merging two data sets from concentrations of 3.91 and 1.95 mg/mL after a 30 s exposure. The radius of gyration ($R_g$) was determined using the Guinier approximation.[30] The pair distribution function [$P(r)$] was calculated using Fourier inversion of scattering intensity $I(q)$ using *GNOM*.[31] $R_g$ was also calculated from the $P(r)$ function. Molecular masses of samples were determined as described previously.[32] Low-resolution molecular envelopes were derived from the scattering profile using *DAMMIF*.[33] Rigid body docking and modeling were performed with *FoXSDock* and *SASREF*[34,35] using atomic coordinates for monoubiquitin [Protein Data Bank (PDB) entry 1UBQ], linear diubiquitin:HOIL1-L-NZF (PDB entry 3BOA), monoubiquitin:UBZ of Wrnip1 (PDB entry 3VHT), and *ab initio* models for Rad18(201−240). The best docked model was chosen using Minimal Ensemble Search (*FoXSMES*).[31,36] Three-dimensional graphics representations were prepared using *PyMOL*.[37]

**Cell Culture, Ionizing Radiation Treatment, and Immunofluorescence Staining.** Mammalian 293T cells were maintained in Dulbecco's modified Eagle's medium (DMEM) supplemented with 10% fetal bovine serum and 5% $CO_2$ (v/v) at 37 °C. Cells expressing EGFP-tagged Rad18 UBZ-ELRM constructs were grown on coverslips and exposed to 10 Gy of infrared (IR) radiation using a JL shepherd $^{137}Cs$ irradiator. Coverslips were stained and imaged with a Leica confocal microscope as previously described.[14,38] Briefly, coverslips containing grown cells were fixed with 3% (v/v) paraformaldehyde at room temperature for 10 min. Cells were permeabilized and blocked with 0.5% (v/v) Triton X-100 and 1% (v/v) goat serum and then incubated with primary antibodies for 60 min at room temperature. Cells were clearly washed with phosphate-buffered saline (PBS) and incubated with an appropriate secondary antibody, rhodamine-conjugated goat anti-rabbit IgG, for 30 min. Images were obtained after a


DOI: 10.1021/bi5012546
*Biochemistry* 2015, 54, 2136−2148

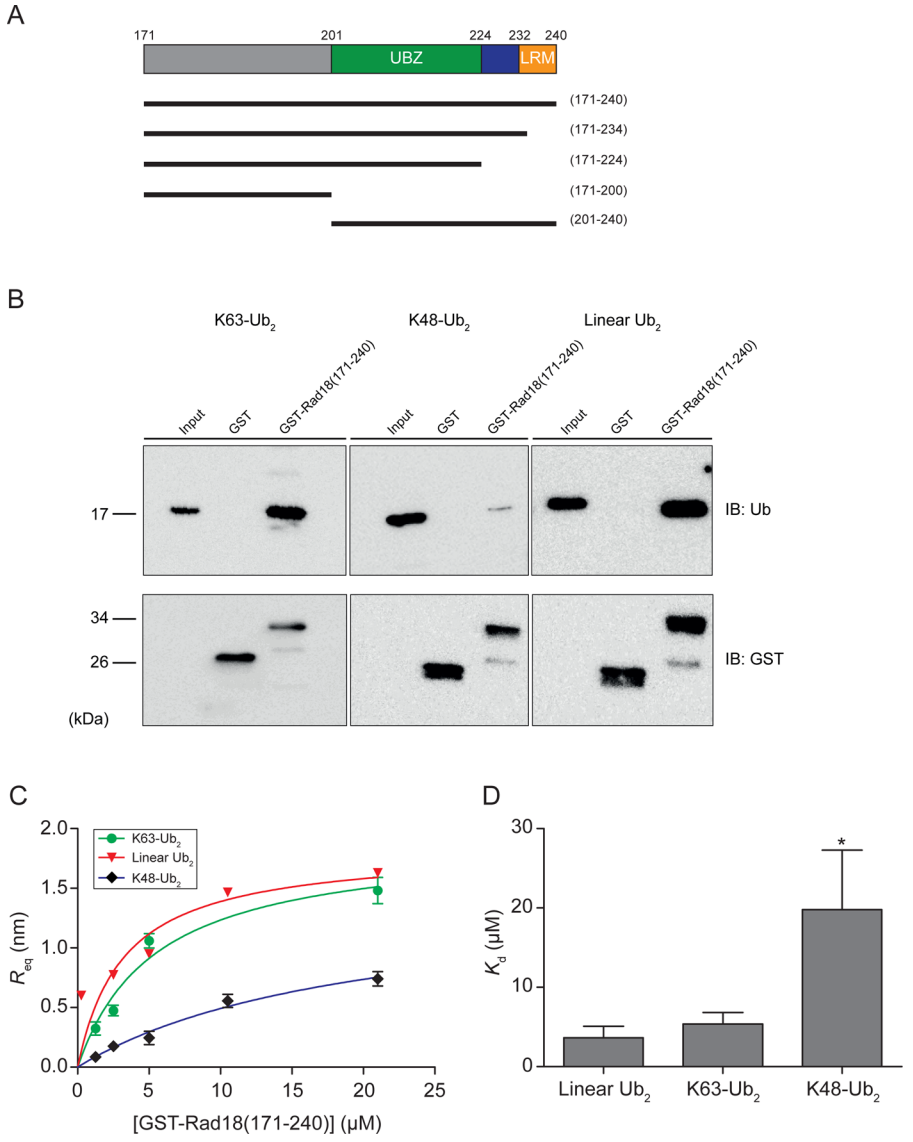


**Figure 1.** Rad18 specifically recognizes linkage-specific polyubiquitin chains. (A) Rad18 constructs were used for this study. Residue numbers for the boundaries of domains and the constructs are displayed. Abbreviations: UBZ, ubiquitin-binding zinc finger domain; LRM, ubiquitylated ligand recognition motif. (B) GST pull-down assays between GST-Rad18(171−240) and K63-linked, K48-linked, and linear $Ub_2$. (C and D) The binding affinity was determined by steady-state fitting of the response at equilibrium ($R_{eq}$) values from BLI experiments.

final washing of the cells with PBS. Cells exhibiting ≥10 foci were recognized as positive foci; ≥50 cells were counted in each experiment. Nuclei were stained with 4,6-diamidino-2-phenylindole (DAPI) (Invitrogen).

**Competitive Ubiquitin Binding Assay.** To monitor competitive binding of Rad18 and RAP80 with linear $Ub_2$, GST pull-down and BLI measurements were performed. Rad18 and RAP80 were permutated in the order of addition to linear $Ub_2$. For GST pull-down experiments, 1 $\mu$M linear His-$Ub_2$ was immobilized on Ni-NTA agarose resin. In the first experiment, 20 $\mu$M Rad18 was added to His-$Ub_2$-loaded Ni-NTA agarose resin and incubated for 2 h at 4 °C while being gently shaken and washed with buffer A to remove unbound proteins. Subsequently, 10 $\mu$M GST-RAP80(60−124) was added to the resin and incubated for 2 h under the same condition described above followed by washing with buffer I. Bound GST-RAP80(60−124) and immobilized His-$Ub_2$ were analyzed by immunoblotting using GST-HRP and His-HRP antibodies. In the second experiment, RAP80(60−124) was preincubated with Ni-NTA agarose resin with the immobilized linear His-$Ub_2$, and then 10 $\mu$M GST-Rad18(171−240) was added to the resin and analyzed by immunoblotting. For BLI experiments, 1 $\mu$M linear His-$Ub_2$ was immobilized on the Ni-NTA sensors. After baseline stabilization with buffer A, 20 $\mu$M Rad18(171−240) was loaded until the signal was saturated. Varying concentrations of GST-RAP80(60−124) were then added and analyzed for competitive binding. In reciprocal experiments, 20 $\mu$M RAP80 was loaded to Ni-NTA sensors with immobilized linear His-$Ub_2$, and then GST-Rad18(171−240) was added. The negative control involved replacing either GST-RAP80(60−124) or GST-Rad18(171−240) with GST.

**Data Analysis.** All data and statistical analyses were performed using *PRISM* (GraphPad Software) and *SigmaPlot* (Systat Software). Differences between data groups were calculated using the two-tail Student's $t$ test and considered significant with a value of $P \leq 0.05$. Results are presented as means and standard deviations from two to four independent experiments.



DOI: 10.1021/bi5012546
*Biochemistry* 2015, 54, 2136−2148

## RESULTS

**Rad18 Recognizes Linear and K63-Linked Diubiquitin Marginally Better Than K48-Linked Diubiquitins.** Rad18 is known to bind both K63-linked and K48-linked pentaubiquitin chains with similar affinities.[13] To dissect ubiquitin binding by Rad18 at the domain level, we generated several Rad18 constructs harboring UBZ and LRM as well as a region at the N-terminus of the UBZ domain (Figure 1A). Because linear polyubiquitin chains are structurally equivalent and function like K63-linked ones,[5,6,38] we included linear polyubiquitin chains as well as K63-linked and K48-linked ones. We asked how GST-Rad18(171−240) differentially recognized linkage-specific diubiquitin chains, considered to be the minimum length for polyubiquitin chains. First, we performed pull-down assays using GST-Rad18(171−240) with either linear $Ub_2$, K63-$Ub_2$, or K48-$Ub_2$. We found that Rad18 bound similarly to linear $Ub_2$ and K63-$Ub_2$, but less favorably to K48-$Ub_2$ (Figure 1B), indicating that GST-Rad18(171−240) apparently prefers binding to linear $Ub_2$ or K63-$Ub_2$. Next, we compared binding affinities of GST-Rad18(171−240) to those of linkage-specific diubiquitin chains determined by BLI. GST-Rad18(171−240) exhibited marginally enhanced binding affinity for K63-$Ub_2$ ($K_d$ = 5.4 ± 1.5 $\mu$M) versus K48-$Ub_2$ ($K_d$ = 19.8 ± 7.5 $\mu$M) but similar affinity for linear $Ub_2$ [$K_d$ = 3.6 ± 1.5 $\mu$M (Table S1 of the Supporting Information and Figure 1C,D)]. Both qualitative and quantitative binding studies showed that GST-Rad18(171−240) preferred to bind to linear and K63-linked diubiquitin instead of a K48-linked one. This observation is in apparent contrast to a previous study in which GST-Rad18(186−240) bound K63-linked and K48-linked pentaubiquitin with similar affinities.[13] However, the preference observed in our study seemed to be marginal because the ratio of binding affinity of Rad18 with a K63-linked polyubiquitin chain to that with a K48-linked one was ∼2 for pentaubiquitin and ∼4 for diubiquitin. The observation that GST-Rad18(171−240) recognizes both linear $Ub_2$ and K63-$Ub_2$ approximately equally is consistent with linear and K63-linked ubiquitin chains having similar structures but both being significantly different from the K48-linked one.[5,6,39,40] Given the similar binding affinities of GST-Rad18(171−240) with linear $Ub_2$ for K63-$Ub_2$, we used linear polyubiquitin chains for further analysis.

**The Extended LRM at the C-Terminus of UBZ Is Important in Polyubiquitin Recognition by Rad18.** To investigate whether Rad18 recognizes linear polyubiquitin in a chain-length-dependent manner and the precise roles of UBZ and LRM in polyubiquitin binding by Rad18, we prepared Ub, linear $Ub_2$, $Ub_3$, and $Ub_4$ and four constructs of GST-Rad18 (residues 171−224, 171−234, 171−240, and 201−240). Pull-down results showed similar affinities with different lengths of linear polyubiquitins regardless of the GST-Rad18 construct used (Figure S1 of the Supporting Information). Consistent with the pull-down assays, quantitative BLI results revealed that binding affinities of GST-Rad18 constructs with linear polyubiquitin chains ($Ub_2$−$Ub_4$) were not statistically significantly different from each other, indicating that chain length may not affect the affinity of Rad18 for polyubiquitin chains (Table 1, Figure 2, and Figure S2 of the Supporting Information). However, we observed moderate enhancements in affinities for polyubiquitin chains in comparison to those for monoubiquitin in GST-Rad18 constructs containing UBZ and residues at its C-terminus (171−234, 171−240, and 201−240). The binding affinity of GST-Rad18(171−224) with monoubiquitin was similar to those with $Ub_2$−$Ub_4$. However, both GST-Rad18(171−234) and GST-Rad18(171−240) exhibited an increase in binding affinities (3.5- and 6-fold, respectively) with linear polyubiquitin chains. By contrast, GST-Rad18(171−200) showed no interaction with ubiquitin at all. These results demonstrate that the region at the C-terminus of UBZ, spanning residues 225−240, termed the "extended LRM" (ELRM), enhances linear polyubiquitin binding affinity. The region at the N-terminus of the UBZ domain (residues 171−200) may facilitate polyubiquitin recognition by Rad18 upon comparison of the binding affinities of GST-Rad18(171−240) and GST-Rad18(201−240).

**Table 1. Binding Affinities of Rad18 Constructs with Linear Polyubiquitin Chains[a]**

| | $K_d$ ($\mu$M) | | | |
|---|---|---|---|---|
| Rad18[b] | Ub | linear $Ub_2$ | linear $Ub_3$ | linear $Ub_4$ |
| 171−240 | 9.1 ± 2.0 | 1.5 ± 0.6 | 1.5 ± 0.1 | 1.4 ± 0.3 |
| 171−234 | 13.5 ± 2.1 | 4.7 ± 1.4 | 6.9 ± 2.3 | 4.3 ± 0.5 |
| 171−224 | 11.2 ± 3.5 | 14.2 ± 1.1 | 10.1 ± 0.1 | 13.6 ± 1.5 |
| 171−200 | nd[c] | nd[c] | nd[c] | nd[c] |
| 201−240 | 4.4 ± 1.1 | 2.2 ± 0.9 | 3.0 ± 0.1 | 2.3 ± 0.4 |

[a]For all measurements, goodness of fit $r^2 \geq 0.90$. [b]GST-Rad18 was used. Numbers indicate construct boundaries. [c]Not determined.

**Table 2. Data Collection and Scattering-Derived Parameters for SAXS Measurements of the Rad18(201−240):Linear $Ub_2$ Complex**

| | |
|---|---|
| **Data Collection** | |
| synchrotron beamline | PAL-4C |
| beam geometry | mica window solid cell/ oscillation capillary |
| wavelength (Å) | 1.24 |
| minimum scattering angle $q$ (deg)[a] | 0.00128 |
| $q$ range (Å$^{-1}$) | 0.009−0.248 |
| exposure time (s) | 30 |
| concentration range (mg/mL) | 0.98−3.91 |
| **Sample Parameters** | |
| purity of sample (%, by SDS−PAGE) | 99 |
| polydispersity (%, by DLS) | 19 |
| temperature (K) | 293.15 |
| **Structural Parameters** | |
| $I(0)$ (cm$^{-1}$) (from Guinier) | 0.0194 ± 0.0002 |
| $R_g$ (Å) (from Guinier) | 20.92 ± 1.38 |
| $I(0)$ (cm$^{-1}$) [from $P(r)$] | 0.0201 ± 0.0001 |
| $R_g$ (Å) [from $P(r)$] | 21.79 ± 0.29 |
| $D_{max}$ (Å) | 68.38 ± 0.28 |
| Porod volume estimate (Å$^3$) | 35592 ± 3659 |
| dry volume calculated from sequence (Å$^3$) | 26198 |
| **Molecular Mass Determination[b]** | |
| $M_r$ (Da) (from *GNOM* file) | 22400 |
| $M_r$ (Da) (from sequence) | 21653 |
| relative discrepancy (%) | 3.5 |
| **Software Used** | |
| primary data reduction | *RAW* |
| data processing | *PRIMUS* |
| *ab initio* analysis | *DAMMIF* |
| validation and averaging | *DAMAVER* |
| three-dimensional presentations | *PyMOL* |

[a]A scattering vector, $q$. [b]Determined from the sample at a concentration of 3.91 mg/mL.



DOI: 10.1021/bi5012546
*Biochemistry* 2015, 54, 2136−2148

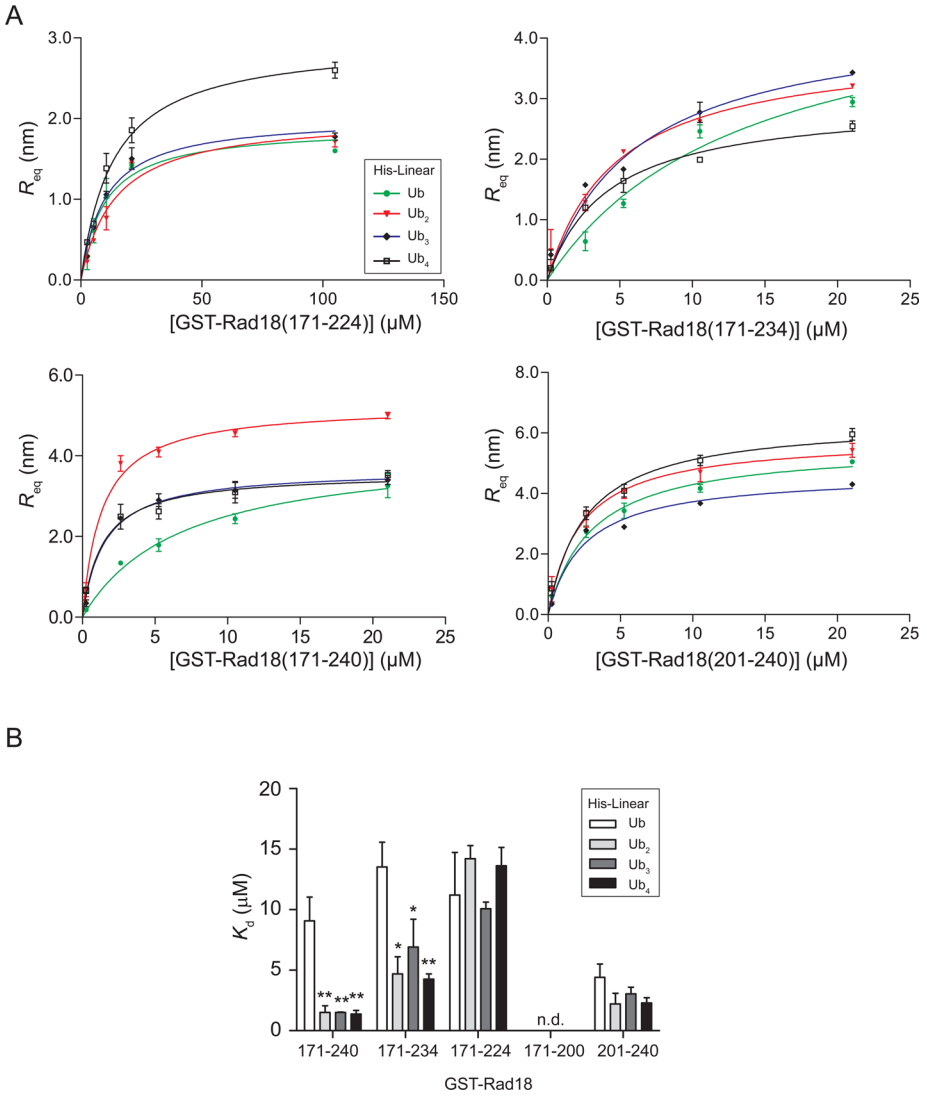


**Figure 2.** Binding affinity between Rad18 constructs and linear polyubiquitin chains. (A) Binding affinity was determined by steady-state fitting of $R_{eq}$ values from BLI experiments. (B) Quantification of $K_d$ from steady-state fitting. The significant difference was analyzed by a Student's $t$ test ($^*P \leq 0.05$; $^{**}P \leq 0.01$).

These results demonstrate that the residues between UBZ and LRM are involved in polyubiquitin recognition by Rad18.

***Ab Initio* Modeling of Rad18(201−240).** To understand the interaction between Rad18 and polyubiquitin at a molecular level, we derived atomic models for the structure of Rad18(201−240) using *GalaxyTMB* and *Rosetta*.[28,29] The two programs yielded similar overall structures: the Rad18(201−240) structural model consists of a UBZ domain and a C-terminal $\alpha$-helix for ELRM ($\alpha$2, residues 227−237) (Figure 3). The UBZ domain contains two short antiparallel $\beta$-strands (residues 201−204 for $\beta$1 and 208−211 for $\beta$2) and an $\alpha$-helix ($\alpha$1, residues 216−224), which packs against the $\beta$-strands with the zinc ion. As with the homologous Wrnip1-UBZ, Rad18-UBZ is classified as a C2HC zinc finger.[17] The derived structural model for the UBZ domain of Rad18 is similar to a recent NMR structure (residues 198−227).[20] In the NMR structure, two $\beta$-strands with a hairpin cover residues 201−211 and the $\alpha$-helix spans residues 212−224. Although the *ab initio* models by the two programs feature the same secondary structural elements, the relative orientation between the UBZ domain and the ELRM helix is slightly different. The ELRM helix from the *GalaxyTBM* model

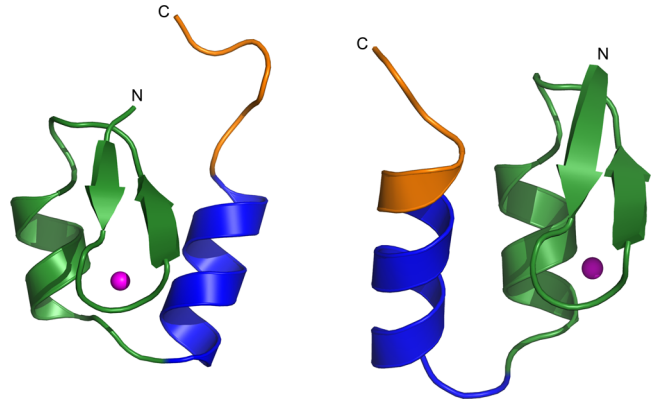


**Figure 3.** *Ab initio* models of the Rad18(201−240) structure. GalaxyTMB (left) and Rosetta (right) *ab initio* models of the Rad18(201−240) structure with regions like the UBZ domain (forest), the region between UBZ domain and the LR motif (blue), and the LR motif (orange). The $Zn^{2+}$ ion is shown as a magenta sphere.

was formed on the right side of the UBZ domain, while it is on the left side in the *Rosetta* model (Figure 3). Another difference



DOI: 10.1021/bi5012546
*Biochemistry* 2015, 54, 2136−2148

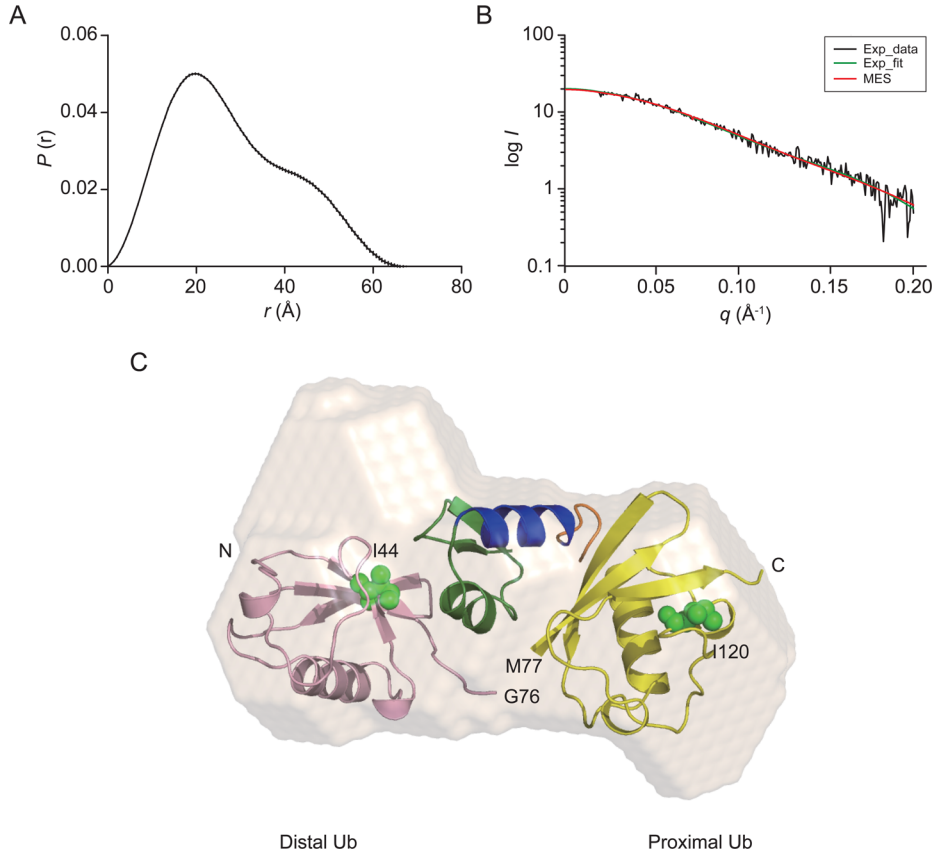


**Figure 4.** Best *ab initio* envelope fitting for the Rad18(201−240):linear $Ub_2$ complex. (A) Pair distribution function of the Rad18(201−240):linear $Ub_2$ complex. (B) Comparison of the experimental scattering profile (black) and minimal ensemble search (red). The minimal ensemble that best fit the experimental data was identified using *FoXSMES*. (C) Best *ab initio* envelope for the Rad18(201−240):linear $Ub_2$ complex.

between the two *ab initio* models is that part of LRM (residues 235−240) is modeled to form a loop by *GalaxyTBM* and an extension of the second helix by *Rosetta* (Figure 3). Nevertheless, our modeling results suggest that ELRM may form a continuous helix. We used both *ab initio* models for Rad18(201−240), generated for SAXS modeling.

**The Low-Resolution Solution Structure of the Rad18:-Linear $Ub_2$ Complex Suggests the Role of ELRM in Proximal Ubiquitin Recognition.** To obtain molecular insights into the interaction between UBZ and ELRM of Rad18 and polyubiquitin in solution, we performed SAXS measurements and derived a molecular envelope for the Rad18(201−240):linear $Ub_2$ complex. Prior to the SAXS measurements, the purity and polydispersity of the Rad18(201−240):linear $Ub_2$ complex were checked by size exclusion chromatography, SDS−PAGE, and DLS (Figure S3 of the Supporting Information). Parameters for SAXS measurements and derivation of low-resolution molecular envelopes for the Rad18(201−240):linear $Ub_2$ complex are summarized in Table 2. The pair distribution functions [$P(r)$] displayed a narrow range, 68.2−68.6 Å (Figure 4A). The $R_g$ determined from Guinier plots was in good agreement with that from *GNOM*. The $R_g$ calculated using *GNOM* ranged from 21.6 to 22.0 Å, supporting the concentration independence of the sample during SAXS measurements. The results indicated that the complex is monomeric and may not be elongated in solution. For *ab initio* modeling of the complex, seven envelopes were generated using *DAMMIF* (Figure S4 of the Supporting Information). The best model fitting with SAXS data was chosen from the lowest $\chi^2$ value ($\chi^2$ = 1.43) using *FoXSMES* (Figure 4B). The rigid body complex was further modeled with *SASREF*.

Because the *FoXSDock* complexes generated no clash between residues and fit the SAXS data with a lower $\chi^2$ value, the Rad18(201−240) model derived from *GalaxyTMB* was used for the SAXS Rad18(201−240):linear $Ub_2$ model. The final molecular envelope with the Rad18(201−240):linear $Ub_2$ complex docked (Figure 4C) revealed that Rad18(201−240) contacts linear $Ub_2$ mainly by its strand $\beta$1 and helix $\alpha$1 in the UBZ domain and the hydrophobic patch centered on I44 of the distal/donor ubiquitin moiety. This is consistent with Rad18-UBZ using the helix and strand $\beta$1 for interaction with the conserved hydrophobic surface on ubiquitin.[20] Additionally, our model suggests that the residues between UBZ and LRM may interact with the proximal/acceptor ubiquitin moiety. This model is consistent with our BLI results showing no difference in binding affinities of GST-Rad18(171−224) (lacking ELRM) with monoubiquitin and linear $Ub_2$.

**Mutational Analysis of the Interaction of Rad18(201−240) with Linear $Ub_2$.** To validate the Rad18(201−240):linear $Ub_2$ complex model derived by SAXS, we prepared nine mutants and assessed their affinities with monoubiquitin and linear $Ub_2$ by BLI: D221A, R226A, E227A, E228A, E231A, V237A, H238A, K239A, and R240A. The D221A mutant, located in the UBZ domain, reportedly abrogates ubiquitin binding.[17,19,20] Four mutants (R226A, E227A, E228A, and E231A) were positioned in the region between UBZ and LRM. R226, E227, and E228 residues are located close to the proximal ubiquitin moiety in our structural model (Figure 5A). E231 is moderately


DOI: 10.1021/bi5012546
*Biochemistry* 2015, 54, 2136−2148

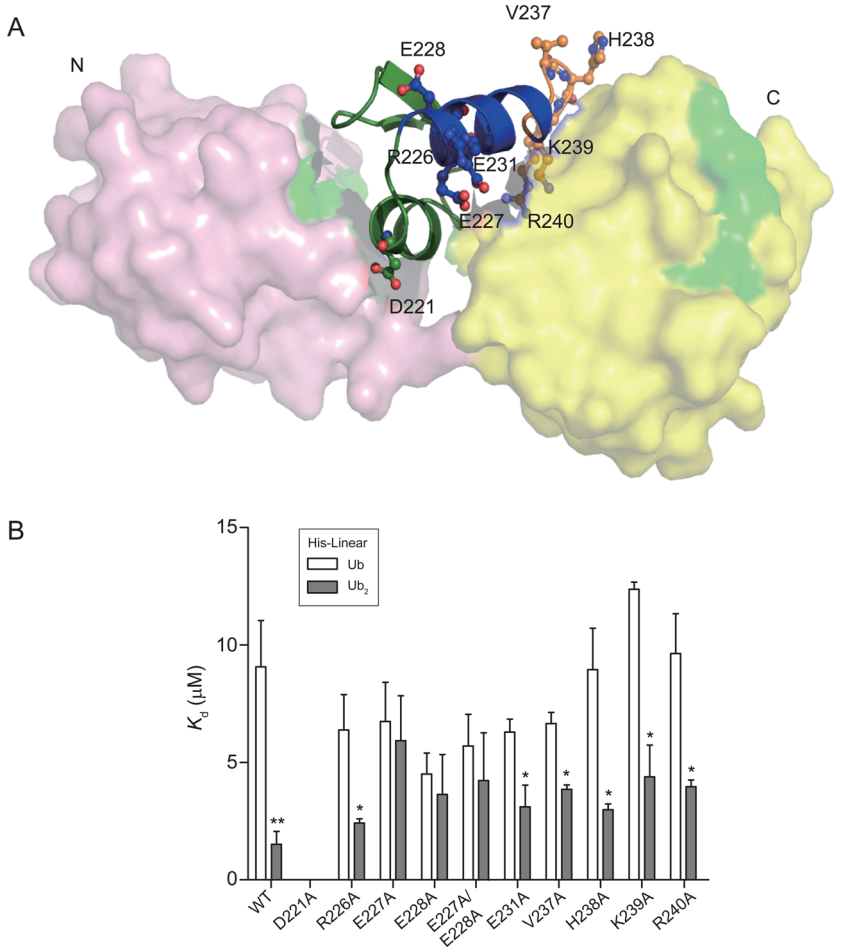


**Figure 5.** Ubiquitin binding affinity of Rad18 mutants. (A) Proposed distribution of mutant residues in the Rad18(201−240):linear $Ub_2$ complex. The I44-centered hydrophobic patch on ubiquitin, which is believed to interact with the ubiquitin-binding domain, is colored green. (B) Binding affinity determined by steady-state fitting of $R_{eq}$ values from BLI experiments.

conserved among the UBZ domains (Figure 5A). Finally, we mutated four C-terminal residues (V237A, H238A, K239A, and R240A) that belong to the LRM (Figure 5A). Quantitative binding analysis showed that all mutants except D221A reduced binding affinities with linear $Ub_2$, but not with monoubiquitin (Figure 5B and Table S2 of the Supporting Information). The D221A mutation showed virtually no interaction with monoubiquitin or linear $Ub_2$, consistent with previous findings,[17,19,20] and our rigid body complex model indicates that D221 interacts with R42 on the distal/donor ubiquitin moiety functioning in complex stabilization (Figure S5A of the Supporting Information). E227A, E228A, and E227A/E228A exhibited similar affinities with linear $Ub_2$ compared with those with monoubiquitin, consistent with our structural model, where E227 interacts with Q78 (corresponding to Q2 in monoubiquitin) of the proximal/acceptor ubiquitin moiety; also, E228 may preserve the structure of the domain (Figure S5B of the Supporting Information). The LRM mutants (V237A, H238A, K239A, and R240A) showed modest decreases in affinities with linear $Ub_2$ but no statistically significant change in affinities with monoubiquitin. This can be explained by the idea that the flexible loop LMR may interact with the proximal/acceptor ubiquitin moiety where K239 and R240 may form hydrogen bonds with D108 [corresponding to D32 in monoubiquitin (Figure S6B of the Supporting Information)]. This supports previous reports that LRM augments binding affinity with polyubiquitin[22] and is consistent with our finding that GST-Rad18(171−234), which lacks the LRM, binds linear polyubiquitin chains less tightly than GST-Rad18(171−240) (Figure 2B). Together, these results establish that ELRM contributes to polyubiquitin recognition by Rad18 and suggest that E227 and E228, located between UBZ and LRM, and the second helix, recognize the proximal/acceptor ubiquitin moiety.

**Polyubiquitin Recognition by ELRM Is Crucial for Rad18 Localization in DNA Damage Sites.** Because the *in vitro* study revealed that E227 and E228 in ELRM are critical in recognizing linear polyubiquitin (Figure 5), we tested whether the aforementioned residues function in localizing Rad18 on DNA damage sites in a cultured cell system. We constructed a plasmid, pEGFP-Rad18(171−240)-SV40NLS, encoding Rad18 UBZ-ELRM (residues 171−240) with EGFP at its N-terminus and SV40 nuclear localization signal at its C-terminus. We introduced the following mutations into the pEGFP-Rad18(171−240)-SV40NLS plasmid: E227A, E228A, or E227A/E228A in ELRM or D221A in the UBZ domain. Expression levels of the transfected plasmids harboring the aforementioned mutations were monitored in 293T cells by immunoblotting with a GFP antibody to ensure similar expression levels among the mutant proteins (Figure S6 of the Supporting Information). The cells were treated with ionizing radiation to test the recruitment of Rad18 UBZ-ELRM to ionizing radiation-induced foci (IRIF). Our results confirmed


DOI: 10.1021/bi5012546
*Biochemistry* 2015, 54, 2136−2148

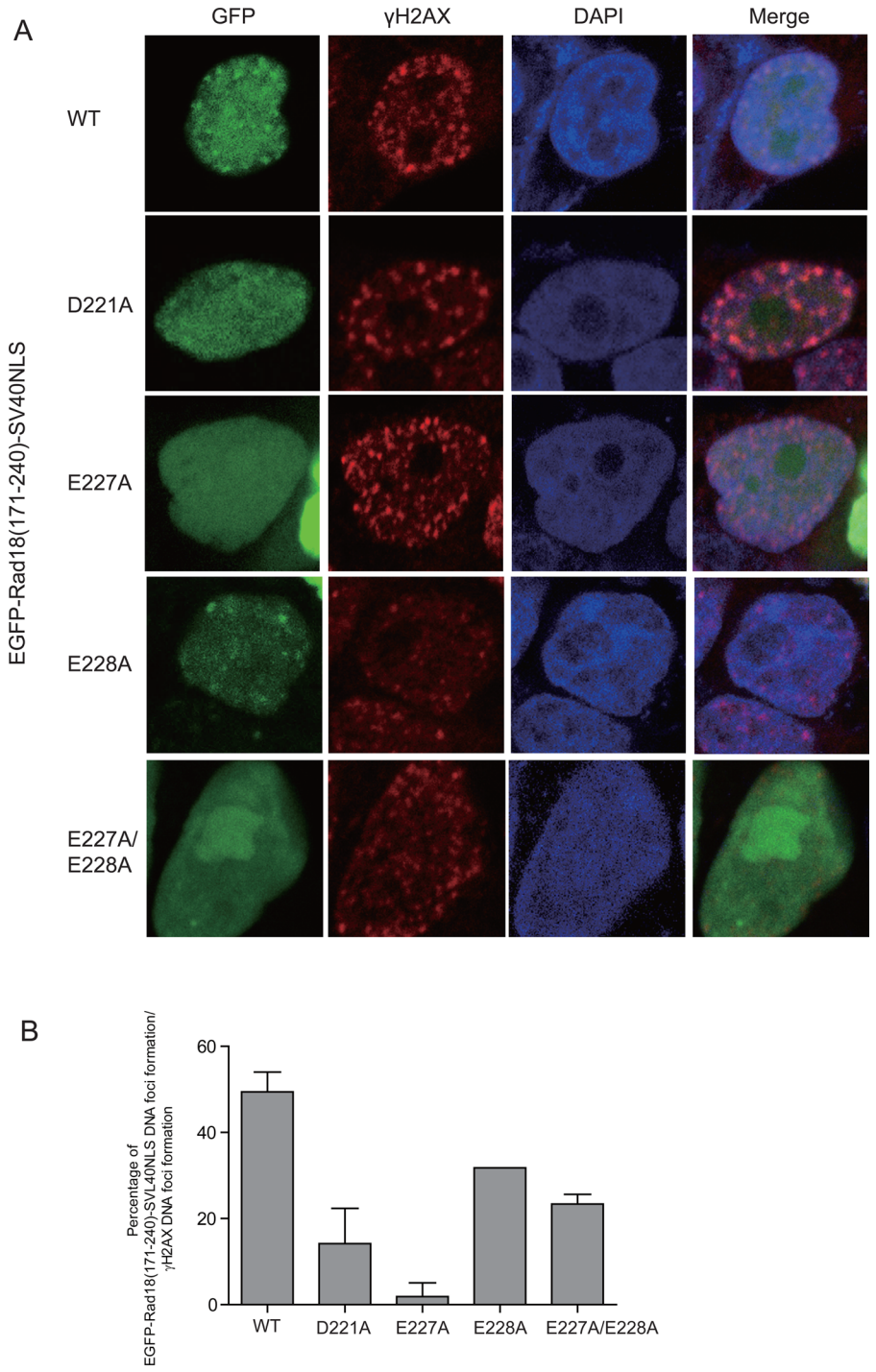


**Figure 6.** ELRM is important in the recruitment of Rad18 to IRIF. (A) Localization of EGFP-Rad18(171−240)-SV40NLS constructs in IRIF 5 h post-10 Gy IR irradiation in mammalian 293T cells. (B) The relative IRIF formation of mutants and WT was quantified. More than 50 cells were counted in each experiment. Standard deviations are shown from duplicate or triplicate experiments.

that the D221A mutant, which was known to be critical in both polyubiquitin recognition and recruitment to IRIF,[14,17] significantly reduced the level of recruitment of Rad18 to IRIF (Figure 6). Compared to the D221A mutant, the E227A mutant also abrogated the recruitment of Rad18 UBZ-ELRM to IRIF similarly or moreso while the E228A mutant reduced it less (Figure 6). Double mutant E227A/E228A also showed a noticeable reduction in the level of recruitment to IRIF. These data are consistent with our *in vitro* polyubiquitin binding data and a structural model in which E227 is likely to make a direct contact with the proximal ubiquitin moiety (Figure 5). Taken together, these results establish that ELRM as well as the UBZ domain is essential in the recruitment of Rad18 to IRIF through specific polyubiquitin recognition.

**Rad18 Outcompetes RAP80 in Linear Polyubiquitin Binding.** In DSB sites, numerous proteins are recruited to initiate the DDR pathway.[22,41] Rad18 and RAP80 play major roles in recruiting other factors during this response by associating with ubiquitylated chromatin through their ubiquitin-binding domains: LRM and two UIMs for RAP80 and UBZ and LRM


DOI: 10.1021/bi5012546
*Biochemistry* 2015, 54, 2136−2148

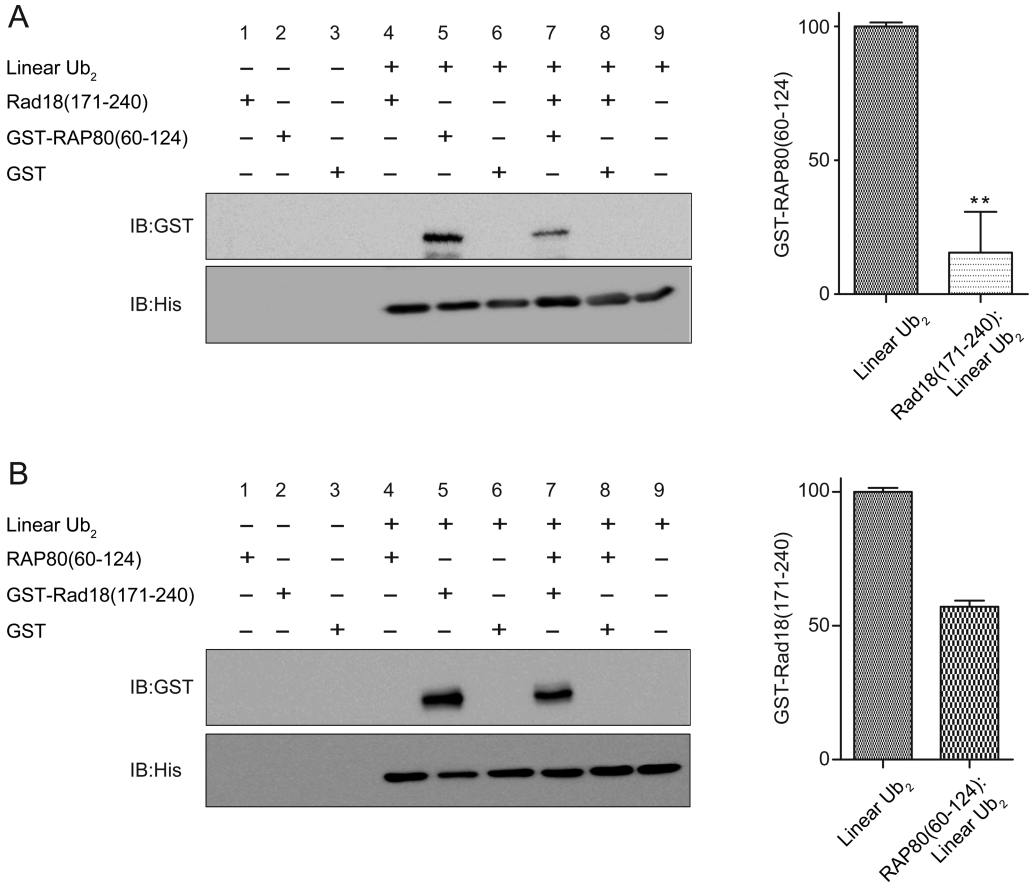


**Figure 7.** Rad18 UBZ-ELRM and RAP80 LRM-UIMs compete for binding with ubiquitin. Rad18(171−240) and RAP80(60−124) were used. (A) Rad18 UBZ-ELRM interferes with the interaction between RAP80 LRM-UIMs and linear $Ub_2$. GST pull-down (left panels) and percentage of band intensity of the ratio between GST-RAP80(60−124) and linear $Ub_2$ in the presence or absence of Rad18(171−240) (right panels). (B) Reciprocal GST pull-down experiments between GST-Rad18(171−240) and linear $Ub_2$ in the presence or absence of RAP80(60−124). Band intensity values were calculated from triplicate experiments.

for Rad18.[22] A previous study reported that overexpressed UBZ of Rad18 interferes with the localization of RAP80 in the nucleus, but not vice versa.[14] To investigate how Rad18 competes with RAP80 in polyubiquitin binding, we examined whether the presence of Rad18 or RAP80 affected binding of the other protein with linear $Ub_2$ *in vitro*, both qualitatively and quantitatively. We immobilized His-linear $Ub_2$ in Ni-NTA resin and analyzed the binding of GST-RAP80(60−124) to linear $Ub_2$ in the absence and presence of Rad18(171−240) (Figure 7A). The level of binding of ubiquitin to GST-RAP80(60−124) decreased in the presence of the preformed Rad18(171−240):linear $Ub_2$ complex (lanes 5 and 7, Figure 7A). By contrast, the presence of the preformed RAP80(60−124):linear $Ub_2$ complex did not significantly interfere with ubiquitin binding of GST-Rad18(171−240) (lanes 5 and 7, Figure 7B).

Quantitative binding analysis using BLI confirmed the results from the GST pull-down assay. First, we checked whether Rad18(171−240) and RAP80(60−124) interacted with each other in the absence of ubiquitin. When Rad18(171−240) was immobilized on a sensor, GST-RAP80(60−124) did not interact with Rad18(171−240) while GST-linear $Ub_4$ did (Figure S7 of the Supporting Information). Next, we immobilized linear $Ub_2$ on a sensor and determined binding affinities of GST-RAP80(60−124) or GST-Rad18(171−240) with linear $Ub_2$ in the presence or absence of Rad18(171−240) or RAP80(60−124), respectively, by BLI (Figure 8A,B). Binding of GST-Rad18(171−240) to linear $Ub_2$ was impaired modestly by the presence of RAP80(60−124), with $K_d$ values being 10.8 ± 4.4 $\mu$M in the presence and 2.7 ± 1.3 $\mu$M in the absence of RAP80 (Table S3 of the Supporting Information). The reciprocal BLI experiments indicated that Rad18(171−240) also perturbed the interaction of GST-RAP80(60−124) with linear $Ub_2$: the binding affinities were 29.5 ± 7.4 and 11.2 ± 6.2 $\mu$M in the presence and absence of Rad18(171−240), respectively (Table S3 of the Supporting Information). Although polyubiquitin binding of both Rad18 and RAP80 was affected by the presence of the other protein, Rad18 appears to bind polyubiquitin more tightly (by ~3-fold) than RAP80 in competitive binding. These results are consistent with a previous study in which overexpression of Rad18 led to blockage of recruitment of RAP80, presumably by interfering with the binding of RAP80 to ubiquitylated chromatin.[22]

## DISCUSSION

In this study, we demonstrated that residues between the UBZ and LRM of Rad18 are also involved in polyubiquitin recognition by biochemical and mutational analyses. We further suggest that the residues between UBZ and LRM are likely to form a continuous helix along with LRM, by SAXS and molecular modeling. Thus, we refer to residues 225−240 as the extended LRM (ELRM). We propose that the ubiquitin-binding domains of Rad18 constitute structurally continuous domains, the UBZ


DOI: 10.1021/bi5012546
*Biochemistry* 2015, 54, 2136−2148

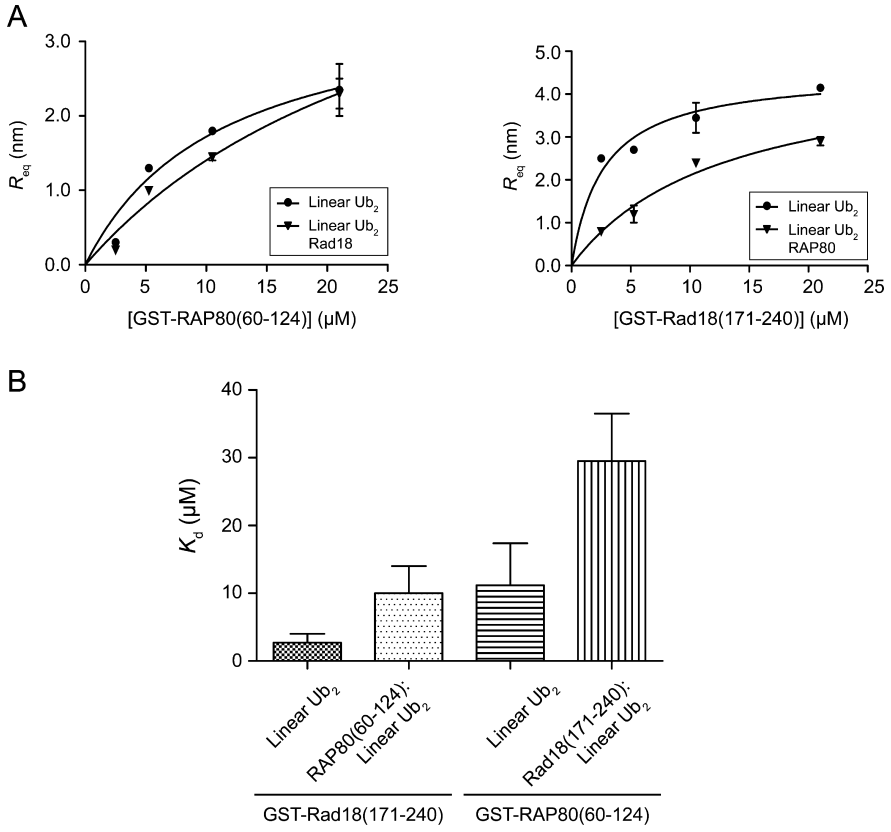


**Figure 8.** Quantitative analysis of competitive binding of Rad18 and RAP80 to polyubiquitin. Binding affinities of linear $Ub_2$ with Rad18(171−240) and RAP80(60−124) in the absence or presence of RAP80(60−124) or Rad18(171−240), respectively. (A) BLI sensorgrams of competitive binding. (B) $K_d$ values determined by steady-state fitting of the data in panel A.

and ELRM. The structural architecture of continuous bipartite ubiquitin-binding domains is not unprecedented. For example, the ubiquitin-binding domains of Rabex-5, an A20-type zinc finger plus MIU, include a continuous helix spanning the C-terminal half of the zinc finger and the whole MIU domain.[42,43] RAP80, also involved in the DDR pathway, features tandem UIM domains connected by a linker.[44,45] The linker between the tandem UIMs of RAP80 has been proposed to become part of a long, continuous helix upon ubiquitin binding.[46,47] RNF168 possesses continuous-helix ubiquitin-binding domains comprising UMI (UIM- and MIU-related) and MIU1 at the N-terminus.[48] This architecture of continuous bipartite ubiquitin domains in a helix might be a common theme in ubiquitin receptors in the DDR pathway.

The accumulation of ubiquitin-binding proteins such as Rad18 in DNA damage sites depends on linkage-specific polyubiquitin recognition.[2,49] It has been proposed that LRM confers specificity to ubiquitin-binding proteins for recruiting their partners as well as an additional source for affinity enhancement toward polyubiquitin.[22] We provide compelling evidence that ELRM, covering residues between the C-terminus of UBZ and LRM, contributes to contacting ubiquitin moieties (Figure 5 and Figure S5 of the Supporting Information). On the basis of our data, we propose differential roles of residues in ELRM in linkage-specific polyubiquitin binding: residues between UBZ and LRM, including E227 and E228, contribute to recognition of the proximal ubiquitin moiety, while those in LRM augment polyubiquitin recognition by their structural plasticity suggested by *ab initio* modeling (Figure 3). However, we cannot rule out the possibility that the interaction between ELRM and ubiquitin may be facilitated by the UBZ domain as well because we could not reliably determine the binding affinity of ELRM alone with monoubiquitin or linear $Ub_2$: the D221A mutant in the UBZ domain totally diminished the level of linear $Ub_2$ binding (Figure 5B). Our *in cell* data reveal that E227A, E228A, and E227A/E228A mutants in ELRM that abrogated binding to linear $Ub_2$ affected recruitment of Rad18 to DNA damage sites (Figure 6). Notably, E227A reduced the level of formation of DNA damage foci more severely than D221A, thereby uncovering the critical role of E227 in the recruitment of Rad18 to DNA damage sites via polyubiquitin recognition. Our *in vitro* and *in cell* data collectively identify novel functional roles of the residues in ELRM in addition to the known function in H2A/X recognition.[22]

A multiple-sequence alignment reveals a substantial difference in ELRM sequences (Figure S8 of the Supporting Information), suggesting that the ELRM may be responsible for conferring specificity in ubiquitin recognition.[22] For example, Rad18 and Wrnip1 share the same bipartite ubiquitin-binding domain architecture (Figure S8 of the Supporting Information). While the UBZ domains in both proteins exhibit a high degree of sequence identity (58%), the ELRMs do not (6%). Such sequence differences in ELRM of Rad18 and Wrnip1 may play a role in differential binding affinities for linkage-specific polyubiquitin recognition: we found Rad18 UBZ-ELRM modestly prefers K63-linked $Ub_2$ to a K48-linked one, whereas Wrnip1 recognizes both with similar affinities.[17] Combining Rad18(201−240) *ab initio* modeling and SAXS data, we found that linear $Ub_2$ is likely to adopt an extended conformation when binding to Rad18. These results suggest that Rad18-ELRM may preferably


DOI: 10.1021/bi5012546
*Biochemistry* 2015, 54, 2136−2148

interact with linear $Ub_2$ or K63-$Ub_2$ (extended conformations, in general[5,6]) more than K48-linked ubiquitin chains (compact conformations[39,50]). Our BLI data also revealed that Rad18-ELRM interacts well with linear $Ub_2$ and K63-$Ub_2$, but less well with K48-$Ub_2$ (Figure 1C vs Figure 1D). Taken together, our data suggest that the ELRM acts as a specificity filter for linkage-specific polyubiquitin chains with the UBZ domain being a generic polyubiquitin binder.

Our data also provide quantitative and molecular bases for the Rad18-dependent redistribution of DDR factors. Binding analysis revealed that Rad18 UBZ-ELRM binds with linear $Ub_2$ more strongly than RAP80 LRM-UIMs, by ~3-fold (Figure 8 and Table S3 of the Supporting Information). However, the affinity is similar in RAP80 LRM-UIMs and Rad18 UBZ alone. Moreover, Rad18 UBZ-ELRM and RAP80 LRM-UIMs compete for binding with polyubiquitin chains, but the interference seems to be stronger in the Rad18 case. Previous *in vivo* results also indicated that overexpression of Rad18 UBZ-ELRM can block the recruitment of RAP80 to DSB sites but RAP80 could not.[14] These findings demonstrate that Rad18 UBZ-ELRM may downregulate recruitment of RAP80 to DSB sites by favorable binding with polyubiquitin chains. BRCA1 is recruited to DSB sites by interaction with the Abraxas:RAP80 complex;[51] thus, it is abrogated by Rad18, too.[14] Together, our results demonstrate that the continuous bipartite ubiquitin-binding domains of Rad18 outcompete RAP80 in polyubiquitin recognition, thereby potentially regulating the DDR pathway.

## ■ ASSOCIATED CONTENT

### Ⓢ Supporting Information

Supplemental tables (S1−S3), supplemental figures (S1−S7), and a supplemental reference. This material is available free of charge via the Internet at http://pubs.acs.org.

## ■ AUTHOR INFORMATION


### Corresponding Author

*Phone: +82-31-290-5913. Fax: +82-31-290-7015. E-mail: sangholee@skku.edu.



### Funding

This work was supported by the Rural Development Agency through the Woo Jang Chun Program (PJ009106), the Basic Science Research Program, through the National Research Foundation of Korea (NRF), funded by the Ministry of Education (NRF-2013R1A1A2059981), and the Pioneer Research Center Program (2012-0009597) through NRF, funded by the Ministry of Science, ICT, and Future Planning.


### Notes

The authors declare no competing financial interest.

## ■ ACKNOWLEDGMENTS


We thank the staff at beamline 4C at the Pohang Accelerator Laboratory for technical assistance in collecting SAXS data and Prof. David Eisenberg and Drs. Duilio Cascio and Lukasz Goldschmidt (University of California, Los Angeles, CA) for access to the Cassini cluster.


## ■ ABBREVIATIONS

DDR, DNA damage response; DSB, DNA double-strand break; UBZ, ubiquitin-binding zinc finger; UIM, ubiquitin-interacting motif; ELRM, extended ligand recognition motif; IRIF, ionizing radiation-induced foci; SAXS, small-angle X-ray scattering; NMR, nuclear magnetic resonance; BLI, biolayer interferometry.

## ■ REFERENCES


(1) Haglund, K., and Dikic, I. (2005) Ubiquitylation and cell signaling. *EMBO J. 24*, 3353−3359.

(2) Jackson, S. P., and Durocher, D. (2013) Regulation of DNA Damage Responses by Ubiquitin and SUMO. *Mol. Cell 49*, 795−807.

(3) Rieser, E., Cordier, S. M., and Walczak, H. (2013) Linear ubiquitination: A newly discovered regulator of cell signalling. *Trends Biochem. Sci. 38*, 94−102.

(4) Chen, Z. J., and Sun, L. J. (2009) Nonproteolytic functions of ubiquitin in cell signaling. *Mol. Cell 33*, 275−286.

(5) Komander, D., and Rape, M. (2012) The ubiquitin code. *Annu. Rev. Biochem. 81*, 203−229.

(6) Komander, D., Reyes-Turcu, F., Licchesi, J. D., Odenwaelder, P., Wilkinson, K. D., and Barford, D. (2009) Molecular discrimination of structurally equivalent Lys 63-linked and linear polyubiquitin chains. *EMBO Rep. 10*, 466−473.

(7) Hurley, J. H., Lee, S., and Prag, G. (2006) Ubiquitin-binding domains. *Biochem. J. 399*, 361−372.

(8) Watanabe, K., Tateishi, S., Kawasuji, M., Tsurimoto, T., Inoue, H., and Yamaizumi, M. (2004) Rad18 guides pol $\eta$ to replication stalling sites through physical interaction and PCNA monoubiquitination. *EMBO J. 23*, 3886−3896.

(9) Shiomi, N., Mori, M., Tsuji, H., Imai, T., Inoue, H., Tateishi, S., Yamaizumi, M., and Shiomi, T. (2007) Human RAD18 is involved in S phase-specific single-strand break repair without PCNA monoubiquitination. *Nucleic Acids Res. 35*, e9.

(10) Ting, L., Jun, H., and Junjie, C. (2010) RAD18 lives a double life: Its implication in DNA double-strand break repair. *DNA Repair 9*, 1241−1248.

(11) van der Laan, R., Uringa, E. J., Wassenaar, E., Hoogerbrugge, J. W., Sleddens, E., Odijk, H., Roest, H. P., de Boer, P., and Hoeijmakers, J. H. (2004) Ubiquitin ligase Rad18Sc localizes to the XY body and to other chromosomal regions that are unpaired and transcriptionally silenced during male meiotic prophase. *J. Cell Sci. 117*, 5023−5033.

(12) Tateishi, S., Niwa, H., Miyazaki, J., Fujimoto, S., Inoue, H., and Yamaizumi, M. (2003) Enhanced genomic instability and defective postreplication repair in RAD18 knockout mouse embryonic stem cells. *Mol. Cell. Biol. 23*, 474−481.

(13) Huang, J., Huen, M. S., Kim, H., Leung, C. C., Glover, J. N., Yu, X., and Chen, J. (2009) RAD18 transmits DNA damage signalling to elicit homologous recombination repair. *Nat. Cell Biol. 11*, 592−603.

(14) Helchowski, C. M., Skow, L. F., Roberts, K. H., Chute, C. L., and Canman, C. E. (2013) A small ubiquitin binding domain inhibits ubiquitin-dependent protein recruitment to DNA repair foci. *Cell Cycle 12*, 3749−3758.

(15) Notenboom, V., Hibbert, R. G., van Rossum-Fikkert, S. E., Olsen, J. V., Mann, M., and Sixma, T. K. (2007) Functional characterization of Rad18 domains for Rad6, ubiquitin, DNA binding and PCNA modification. *Nucleic Acids Res. 35*, 5819−5830.

(16) Miyase, S., Tateishi, S., Watanabe, K., Tomita, K., Suzuki, K., Inoue, H., and Yamaizumi, M. (2005) Differential regulation of Rad18 through Rad6-dependent mono- and polyubiquitination. *J. Biol. Chem. 280*, 515−524.

(17) Crosetto, N., Bienko, M., Hibbert, R. G., Perica, T., Ambrogio, C., Kensche, T., Hofmann, K., Sixma, T. K., and Dikic, I. (2008) Human Wrnip1 is localized in replication factories in a ubiquitin-binding zinc finger-dependent manner. *J. Biol. Chem. 283*, 35173−35185.

(18) Doil, C., Mailand, N., Bekker-Jensen, S., Menard, P., and Larsen, D. H. (2009) RNF168 binds and amplifies ubiquitin conjugates on damaged chromosomes to allow accumulation of repair proteins. *Cell 136*, 435−446.

(19) Inagaki, A., Sleddens-Linkels, E., van Cappellen, W. A., Hibbert, R. G., Sixma, T. K., Hoeijmakers, J. H., Grootegoed, J. A., and Baarends, W. M. (2011) Human RAD18 interacts with ubiquitylated chromatin components and facilitates RAD9 recruitment to DNA double strand breaks. *PLoS One 6*, e23155.

(20) Rizzo, A. A., Salerno, P. E., Bezsonova, I., and Korzhnev, D. M. (2014) NMR structure of the human Rad18 zinc finger in complex




DOI: 10.1021/bi5012546
*Biochemistry* 2015, 54, 2136−2148

with ubiquitin defines a class of UBZ domains in proteins linked to the DNA damage response. *Biochemistry 53*, 5895−5906.
(21) Bomar, M. G., Pai, M. T., Tzeng, S. R., Li, S. S., and Zhou, P. (2007) Structure of the ubiquitin-binding zinc finger domain of human DNA Y-polymerase *η*. *EMBO Rep. 8*, 247−251.
(22) Panier, S., Ichijima, Y., Fradet-Turcotte, A., Leung, C. C., Kaustov, L., Arrowsmith, C. H., and Durocher, D. (2012) Tandem protein interaction modules organize the ubiquitin-dependent response to DNA double-strand breaks. *Mol. Cell 47*, 383−395.
(23) Sheffield, P., Garrard, S., and Derewenda, Z. (1999) Overcoming Expression and Purification Problems of RhoGDI Using a Family of "Parallel" Expression Vectors. *Protein Expression Purif. 15*, 34−39.
(24) Wu, X., Wu, D., Lu, Z., Chen, W., Hu, X., and Ding, Y. (2009) A Novel Method for High-Level Production of TEV Protease by Superfolder GFP Tag. *J. Biomed. Biotechnol. 2009*, 8.
(25) Bradford, M. M. (1976) A rapid and sensitive method for the quantitation of microgram quantities of protein utilizing the principle of protein-dye binding. *Anal. Biochem. 72*, 248−254.
(26) Pickart, C. M., and Raasi, S. (2005) Controlled Synthesis of Polyubiquitin Chains. In *Methods in Enzymology* (Raymond, J. D., Ed.) pp 21−36, Academic Press, San Diego.
(27) Dong, K. C., Helgason, E., Yu, C., Phu, L., Arnott, D. P., Bosanac, I., Compaan, D. M., Huang, O. W., Fedorova, A. V., Kirkpatrick, D. S., Hymowitz, S. G., and Dueber, E. C. (2011) Preparation of distinct ubiquitin chain reagents of high purity and yield. *Structure 19*, 1053−1063.
(28) Ko, J., Park, H., Heo, L., and Seok, C. (2012) GalaxyWEB server for protein structure prediction and refinement. *Nucleic Acids Res. 40*, W294−W297.
(29) Raman, S., Vernon, R., Thompson, J., Tyka, M., Sadreyev, R., Pei, J., Kim, D., Kellogg, E., DiMaio, F., Lange, O., Kinch, L., Shffler, W., Kim, B.-H., Das, R., Grishin, N. V., and Baker, D. (2009) Structure prediction of CASP8 with all-atom refinement using Rosetta. *Proteins 77*, 89−99.
(30) Guinier, A. F., and Fournet, F. (1955) *Small Angle X-rays*, Wiley Interscience, New York.
(31) Pelikan, M., Hura, G. L., and Hammel, M. (2009) Structure and flexibility within proteins as identified through small angle X-ray scattering. *Gen. Physiol. Biophys. 28*, 174−189.
(32) Fischer, H., Oliveira Neto de, M., Napolitano, B. H., Polikarpov, I., and Craievich, F. A. (2010) Determination of the molecular weight of proteins in solution from a single small-angle X-ray scattering measurement on a relative scale. *J. Appl. Crystallogr. 43*, 101−109.
(33) Franke, D., and Svergun, D. I. (2009) DAMMIF, a program for rapid ab-initio shape determination in small-angle scattering. *J. Appl. Crystallogr. 42*, 342−346.
(34) Schneidman-Duhovny, D., Hammel, M., and Sali, A. (2010) Macromolecular docking restrained by a small angle X-ray scattering profile. *J. Struct. Biol. 173*, 461−471.
(35) Petoukhov, M. V., and Svergun, D. I. (2005) Global rigid body modelling of macromolecular complexes against small-angle scattering data. *Biophys. J. 89*, 1237−1250.
(36) Schneidman-Duhovny, D., Hammel, M., Tainer, J. A., and Sali, A. (2013) Accurate SAXS profile computation and its assessment by contrast variation experiments. *Biophys. J. 105*, 962−974.
(37) DeLano, W. L. (2002) *The PyMOL Molecular Graphics System*, DeLano Scientific LLC, San Carlos, CA.
(38) Cho, H. J., Lee, S., and Kim, H. (2009) The linker connecting the tandem ubiquitin binding domains of RAP80 is critical for lysine 63-linked polyubiquitin-dependent binding activity. *BMB Rep. 42*, 764−768.
(39) Satoh, T., Sakata, E., Yamamoto, S., Yamaguchi, Y., Sumiyoshi, A., Wakatsuki, S., and Kato, K. (2010) Crystal structure of cyclic Lys48-linked tetraubiquitin. *Biochem. Biophys. Res. Commun. 400*, 329−333.
(40) Ye, Y., Blaser, G., Horrocks, M. H., Ruedas-Rama, M. J., Ibrahim, S., Zhukov, A. A., Orte, A., Klenerman, D., Jackson, S. E., and Komander, D. (2012) Ubiquitin chain conformation regulates recognition and activity of interacting proteins. *Nature 492*, 266−270.
(41) Bao, Y. (2011) Chromatin response to DNA double-strand break damage. *Epigenomics 3*, 307−321.
(42) Lee, S., Tsai, Y. C., Mattera, R., Smith, W. J., Kostelansky, M. S., Weissman, A. M., Bonifacino, J. S., and Hurley, J. H. (2006) Structural basis for ubiquitin recognition and autoubiquitination by Rabex-5. *Nat. Struct. Mol. Biol. 13*, 264−271.
(43) Penengo, L., Mapelli, M., Murachelli, A. G., Confalonieri, S., Magri, L., Musacchio, A., Di Fiore, P. P., Polo, S., and Schneider, T. R. (2006) Crystal structure of the ubiquitin binding domains of rabex-5 reveals two modes of interaction with ubiquitin. *Cell 124*, 1183−1195.
(44) Sato, Y., Yoshikawa, A., Mimura, H., Yamashita, M., Yamagata, A., and Fukai, S. (2009) Structural basis for specific recognition of Lys 63-linked polyubiquitin chains by tandem UIMs of RAP80. *EMBO J. 28*, 2461−2468.
(45) Sims, J. J., and Cohen, R. E. (2009) Linkage-specific avidity defines the lysine 63-linked polyubiquitin-binding preference of rap80. *Mol. Cell 33*, 775−783.
(46) Sekiyama, N., Jee, J., Isogai, S., Akagi, K., Huang, T. H., Ariyoshi, M., Tochio, H., and Shirakawa, M. (2012) NMR analysis of Lys63-linked polyubiquitin recognition by the tandem ubiquitin-interacting motifs of Rap80. *J. Biomol. NMR 52*, 339−350.
(47) Thach, T. T., Jee, J., and Lee, S. (2012) Effects of a phosphomimetic mutant of RAP80 on linear polyubiquitin binding probed by calorimetric analysis. *Bull. Korean Chem. Soc. 33*, 1285−1289.
(48) Pinato, S., Gatti, M., Scandiuzzi, C., Confalonieri, S., and Penengo, L. (2011) UMI, a novel RNF168 ubiquitin binding domain involved in the DNA damage signaling pathway. *Mol. Cell. Biol. 31*, 118−126.
(49) Panier, S., and Durocher, D. (2013) Push back to respond better: Regulatory inhibition of the DNA double-strand break response. *Nat. Rev. Mol. Cell Biol. 14*, 661−672.
(50) Lai, M. Y., Zhang, D., Laronde-Leblanc, N., and Fushman, D. (2012) Structural and biochemical studies of the open state of Lys48-linked diubiquitin. *Biochim. Biophys. Acta 1823*, 2046−2056.
(51) Wang, B., Matsuoka, S., Ballif, B. A., Zhang, D., Smogorzewska, A., Gygi, S. P., and Elledge, S. J. (2007) Abraxas and RAP80 form a BRCA1 protein complex required for the DNA damage response. *Science 316*, 1194−1198.


DOI: 10.1021/bi5012546
*Biochemistry* 2015, 54, 2136−2148